Postprint of: Łukasik N., Wagner-Wysiecka E., Anion binding by p-aminoazobenzene-derived aromatic amides: spectroscopic and electrochemical studies, PHOTOCHEMICAL & PHOTOBIOLOGICAL SCIENCES, Vol. 16, Iss. 10 (2017), pp. 1570-1579, DOI: 10.1039/c7pp00245a

# ANION BINDING BY *P*-AMINOAZOBENZENE-DERIVED AROMATIC AMIDES: SPECTROSCOPIC AND ELECTROCHEMICAL STUDIES†

Natalia Łukasik* and Ewa Wagner-Wysiecka*

Department of Chemistry and Technology of Functional Materials, Faculty of Chemistry, Gdansk University of Technology, Narutowicza Street 11/12, 80-233 Gdańsk, Poland.

E-mail: natalia.lukasik@pg.gda.pl, ewa.wagner-wysiecka@pg.gda.pl

†Electronic supplementary information (ESI) available. See DOI: 10.1039/ c7pp00245a

The synthesis and complexing properties of *p*-aminoazobenzene-derived mono-, bis-, and trisamides were described. Ligands **3** and **4** bind anions, including fluorides, chlorides, bromides, acetates, benzoates, dihydrogen phosphates, hydrogen sulfates, and *p*-toluenesulfonates, in chloroform forming 1 : 1 complexes. The highest value of stability constant was evaluated for the **4**-$F^-$ complex (log $K$ = 5.63 ± 0.21). On the basis of $^1$H NMR, and FTIR spectroscopy, the possible nature of the ligand–anion interactions was proposed. The $E \rightleftarrows Z$ isomerization process of tripodal amide **4** in chloroform was studied. The effect of anions on $Z$ to $E$ thermal back isomerization was investigated.

## Introduction

For years one of the most active fields of supramolecular chemistry has been the design, synthesis, and study of the complexing properties of organic compounds acting as host molecules for negatively charged guests.[1] Appropriate anion receptors can find a vast variety of applications, including in anion separation from industrial and radioactive waste,[2] in the development of anion sensors working under real-world conditions[3] or in catalysis where ligand–anion interaction is crucial for reaction effectiveness.[4] In analytical supramolecular chemistry, relatively simple molecules enabling selective anion detection can be successfully used.[5] Important structural features of receptors are binding sites and signalling units, thanks to which chemical information is converted into a useful, e.g. optical or electrical, signal. Incorporation into the ligand structure of several groups

of different character allows molecular recognition to be studied through various analytical methods providing more detailed information on the nature and mechanism of host–guest interactions. Unique in this respect are azocompounds, which have been known for more than 100 years. These compounds are still of high interest due to their efficient methods of synthesis[6] and interesting properties, such as photo and redox activity,[7] enabling their application in various fields from materials science to neurobiology.

For example, an azo moiety is often incorporated into macrocyclic compounds acting as a host molecule for metal cations.[8] On the other hand, decoration of proteins with an azobenzene unit enabled photoswitchable $K^+$ channels,[9] GABA receptors[10] and transcription factors to be obtained.[11] Photoisomerization of azocompounds is also often used in the development of photo-responsive smart polymers, information storage materials, and molecular machines.[12]

Taking into account the high importance of anion recognition and interesting properties of azocompounds, we decided to synthesize a series of simple compounds bearing one, two or three amide moieties and azo residues. We expect that the combination of H-bond donating amide residue(s) and azo group(s) in one molecule will result in receptors enabling optical and electrochemical anion sensing. The skeleton of the receptors proposed here is based on an aromatic platform: a benzene or pyridine ring. The ion binding, optical, and electrochemical properties of the obtained ligands are described.

## Experimental section

### General considerations

All chemicals of the highest available purity were purchased from commercial sources and used without further purification. The reaction progress was monitored by TLC using aluminium sheets covered with silica gel $60F_{254}$ (Merck). NMR spectra in DMSO-$d_6$ and chloroform-$d$ were recorded on Varian apparatus at 200 or 500 MHz for $^1H$ and 125 MHz for $^{13}C$. Chemical shifts are reported as δ [ppm] values in relation to TMS. FTIR spectra were recorded on Nicolet iS10 apparatus.

UV-Vis titrations in DMSO (Sigma-Aldrich) or chloroform (StanLab, distilled before use) were carried out using a UNICAM UV 300 spectrophotometer. For spectrophotometric measurements, 1 cm quartz cuvettes were used. Cyclic voltammetry was performed

on an AUTOLAB 302N potentiostat–galvanostat (AUTOLAB, Eco Chemie, B.V., Netherlands) using GEPS Manager software. The electrochemical experiments were carried out with the use of a conventional three-electrode cell consisting of a glassy carbon working electrode, a platinum wire counter electrode, and an Ag|AgCl|0.1 M KCl reference electrode. Disc shaped glassy carbon electrodes (2 mm) were purchased form MINERAL (Warsaw, Poland). UV irradiation experiments were carried out in a chamber equipped with a UVA lamp (Spectroline, model ENF-240C/FE, 4 W, $\lambda_{max}$ = 365 nm).

**Synthesis**

The carboxamides **1–4** were prepared using a simple synthetic method.[13] The appropriate acid chloride (benzoic, pyridine2,6-dicarboxylic, isophthalic or trimesic, 1 mmol) was added stepwise to a solution of 4-aminoazobenzene (1, 2 or 3 mmol for obtainment of amide **1** or **2** and **3** or **4** respectively, Fig. 1) and triethylamine (1, 2 or 3 mmol) in 10 mL of dimethylformamide (DMF). The reaction mixture was magnetically stirred for 16 hours at 60 °C. To the cooled reagents, water was added and the precipitate was filtrated off. Pure products were obtained after crystallization from ethyl acetate or methanol.

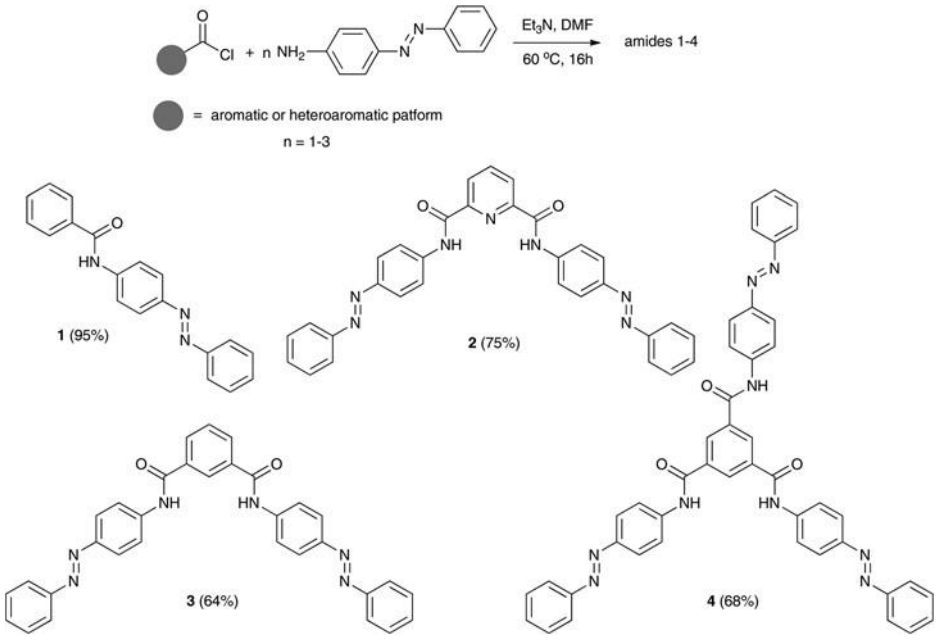


**Fig. 1** Synthesis of compounds **1–4**. UV-Vis ($CHCl_3$): $\lambda_{max}(\varepsilon)$ = 350 nm ($1.4 \times 10^4$), 434 nm ($1.4 \times 10^3$).

Compound 1: Yield 95% (0.28 g), lit. 90%, mp. 202–204°C,[14] orange solid, $R_f$ = 0.92 ($CH_2Cl_2$ : MeOH 15 : 1); mp. = 203–204 °C; IR (KBr pellet) $cm^{-1}$: 3369, 3056, 1665, 1601, 1526,

843, 688; $^1$H NMR (200 MHz, DMSO-$d_6$, δ [ppm]), E-isomer: 7.53–7.64 (5H, m); 7.86–7.97 (9H, m); 10.60 (1H, s);

Compound 2: Yield 75% (0.39 g), orange solid, $R_f$ = 0.84 ($CHCl_3$ : acetone 10 : 1), mp. >300°C, IR (nujol) cm$^{-1}$: 3250, 1673, 1662, 1539, 1239, 1151, 1106, 999, 838, 766, 685; $^1$H NMR (500 MHz, DMSO-$d_6$, δ [ppm]), all-E isomer: 7.58–7.62 (6H, m); 7.92 (4H, d, J = 7.3 Hz); 8.05 (4H, d, J = 8.8 Hz); 8.25 (4H, d, J = 8.8 Hz); 8.39 (1H, t, J = 7.8 Hz); 8.48 (2H, d, J = 7.8 Hz); 11.35 (2H, s); $^{13}$C NMR (125 MHz, DMSO-$d_6$, δ [ppm]): 121.82, 123.12, 124.31, 126.47, 130.16, 131.94, 140.90, 141.85, 148.94, 149.31, 152.74, 162.66; UV-Vis ($CHCl_3$): $\lambda_{max}(\varepsilon)$ = 351 nm ($5.4 \times 10^4$), 440 nm ($3.7 \times 10^3$); HRMS(EI): 525.19023 for formula $C_{31}H_{23}N_7O_2$, calculated: 525.19132.

Compound 3: Yield 64% (0.34 g) orange solid, mp. >300 °C; $R_f$ = 0.89 ($CHCl_3$ : acetone 10 : 1), IR (KBr pellet) cm$^{-1}$: 3274, 3063, 1649, 1598, 1528, 1406, 686; $^1$H NMR (500 MHz, DMSO-$d_6$, δ [ppm]), all-E isomer: 7.55 (2H, t, J = 3.7 Hz), 7.58 (4H, t, J = 7.3 Hz), 7.74 (1H, t, J = 7.8 Hz), 7.87 (4H, d, J = 7.3 Hz), 7.95 (4H, d, J = 8.8 Hz), 8.06 (4H, d, J = 8.8 Hz), 8.20 (2H, d, J = 7.8 Hz), 8.60 (1H, s), 10.80 (2H, s); UV-Vis ($CHCl_3$): $\lambda_{max}(\varepsilon)$ = 352 nm ($3.3 \times 10^4$), 434 nm ($2.3 \times 10^3$).

Compound 4: Yield 68% (0.51 g), lit. 70%, mp. 317 °C,[15] orange solid, $R_f$ = 0.56 ($CH_3Cl$ : acetone 10 : 1), mp. >300 °C, IR (KBr pallet) cm$^{-1}$: 3431, 3063, 1677, 1596, 1533, 1405, 687; $^1$H NMR (500 MHz, DMSO-$d_6$, δ [ppm]), all-E isomer: 7.50–7.68 (9H, m); 7.89 (6H, d, J = 7.1 Hz); 7.99 (6H, d, J = 9.1 Hz); 8.11 (6H, d, J = 8.9 Hz); 8.83 (3H, s); 10.97 (3H, s); UV-Vis ($CHCl_3$): $\lambda_{max}(\varepsilon)$ = 353 nm ($8.3 \times 10^4$), 437 nm ($5.3 \times 10^3$).

**Ligand–ion interaction studies**

The binding properties of the obtained amides were tested using UV-Vis spectrophotometry, $^1$H NMR, and FTIR spectroscopy. In complexation studies, many metal cations (alkali, alkaline earth, and heavy divalent metal cations) in the form of perchlorate salts as well as anions of different sizes and shapes (as tetra-*n*-butylammonium (TBA) salts) were used. Spectrophotometric titrations were carried out in DMSO, acetonitrile or chloroform. On the basis of experimental data, the stability constant values and stoichiometry of formed species were determined using OPIUM software.[16] Molecular models of amides **3** and **4** were calculated using the MM:UFF method with ArgusLab software.[17] In the $^1$H NMR experiments, DMSO-$d_6$

or chloroform-*d* as a solvent was used. In the voltammetric experiments, the electrolyte – 0.1 M tetra-*n*-butylammonium perchlorate – was initially purged with argon for 40 min in order to remove oxygen. All electrochemical tests were performed under argon atmosphere. The cyclic voltammetry curves were registered for the "free" ligand **4** solution ($c_4 = 2.48 \times 10^{-4}$ M) and after addition of a 100-fold molar excess of the respective TBA salt solution in acetonitrile with a scan rate of 50 mV $s^{-1}$.

**Photoisomerization process studies**

The photostationary state was obtained after 3 minutes of irradiation of the ligand **4** solution ($c_4 = 2.01 \times 10^{-5}$ M) in chloroform placed in a quartz cuvette (l = 1 cm) with ultraviolet light (365 nm). The progress of the photoisomerization process was monitored using UV-Vis spectrophotometry. *Z* to *E* back isomerization was conducted at 50 °C in the dark.

## Results and discussion

Amides **1–4** were prepared as shown in Fig. 1 using *p*-aminoazobenzene and the respective acid chloride as substrates. Compounds **1**, **3**, and **4** are known in the literature; however, their ion binding properties have not been studied before. Synthesis of compound **3** was described in a US patent;[18] however, neither its spectral characteristics nor its complexing properties were described. Tripodal amide **4** was tested in photoinduced mass transport processes.[15] To the best of our knowledge (according to Chemical Abstracts), amide **2** is a new compound and has not been described in the literature before. As presented here, a simple synthetic method can serve as a facile procedure for amide synthesis with a satisfactory yield (64–95%).

Amides, due to the presence of an NH group, can serve as potential anion receptors. Ion–ligand interactions for compounds **1–4** reported here were studied using UV-Vis spectrophotometry in solvents of different polarity: DMSO, acetonitrile and chloroform.

In dipolar DMSO, changes in the UV-Vis spectra of ligands **1–4** were observed only in the presence of tetra-*n*-butylammonium hydroxide (TBAOH) and highly basic fluorides (TBAF) among all the tested anions of different sizes and shapes. No spectral changes were observed in the presence of metal cations (as perchlorate salts). Addition of TBAF or TBAOH to the ligand solutions caused a large bathochromic shift of the ligand absorption band and a change in color from yellow to intensive orange. This indicates that ligand

deprotonation may be the dominant process, as fluoride and hydroxide ions are strong bases in polar DMSO. Lee *et al.*[19] reported that addition of a fluoride salt to an aqueous DMSO solution of ligand **4** caused destruction of the microfiber morphology existing under such conditions (10 mM, DMSO : H2O 1 : 1 v/v), which is a result of compound deprotonation. In our studies, only for ligand **2** (the derivative of pyridine-2,6-dicarboxylic acid) changes observed in the spectrum upon titration with TBAF solution indicate more complex behavior than just deprotonation (Fig. 2a). It is possible that in the initial phase of titration, fluoride anions are coordinated by ligand **2**; however, a higher concentration of the salt causes ligand deprotonation, which is indicated by the appearance of a characteristic triplet at 16.20 ppm in the $^{1}$H NMR spectrum (ESI: Fig. ESI1†). The stoichiometry of the species formed during the initial stage of spectrophotometric titration is 1 : 2 (ligand to salt, obtained from the molar ratio plot). A change of solvent to the less polar acetonitrile (in which the fluoride anion is a weaker base than in DMSO) decreases the probability of deprotonation. Under these conditions, the system with compound **2** equilibrates at a 2-fold molar excess of the salt in relation to the ligand, indicating $F_2L$ type stoichiometry (Fig. 2b).

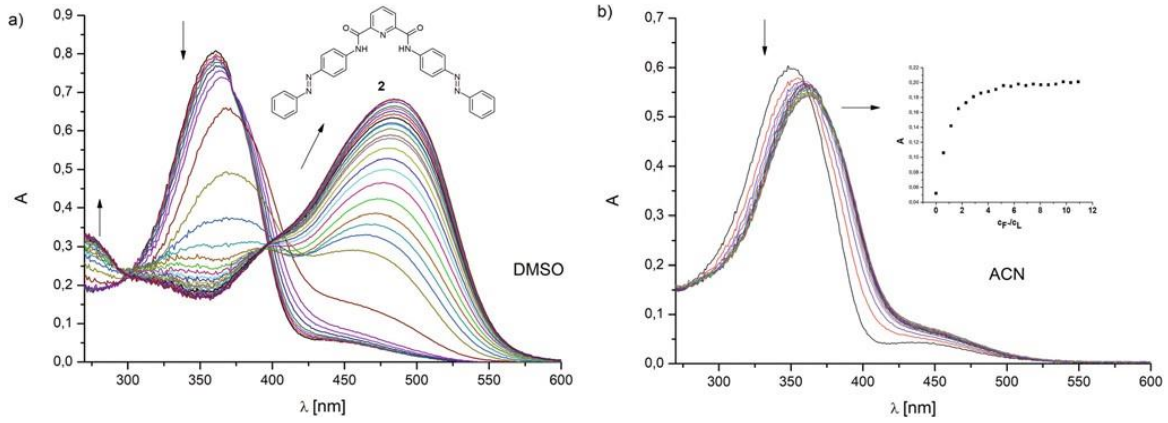


**Fig. 2** Changes in the UV-Vis spectra upon titration of ligand **2** (a) in DMSO ($c_2$ = 1.49 × $10^{-5}$ M, 0 ≤ R ≤ 40.10) and (b) in acetonitrile ($c_2$ = 1.24 × $10^{-5}$ M, 0 ≤ R ≤ 10.91) with tetra-*n*-butylammonium fluoride; *R* = salt/ligand molar ratio; inset: molar ratio plot.

The interactions of ligands **1–4** with anions were also investigated in chloroform. A solvent of low polarity is less competitive in the process of host–guest recognition, which may have a positive influence on the strength of ligand–ion interactions. Although ligands

capable of selective analyte binding in aqueous solutions are highly desirable, the use of a less polar solvent is also useful as it may to some extent reflect the processes occurring in hydrophobic membranes. In order to test the complexing properties of amides **1–4** in chloroform, the influence of metal cations and anions of different sizes and shapes on the ligand absorption spectra was studied. No significant spectral changes were observed upon titration of ligands **1–4** with metal perchlorates. TBA salts also caused no changes in the spectra of amide **1** and **2** solutions. This is opposite to amides **3** and **4** – derived from isophthalic and trimesic acids – which showed a response towards anions, including fluoride, chloride, bromide, acetate, benzoate, dihydrogen phosphate, hydrogen sulfate, and *p*-toluenesulfonate. Moreover, ligand **4** also exhibits the ability to bind nitrate anions. In the UV-Vis spectra of the ligand solutions, a bathochromic shift upon TBA salt addition was observed, which was accompanied by a deepening of the ligand solution color. As an example, in Fig. 3, a comparison of the spectrophotometric titration traces for ligands **3** and **4** with dihydrogen phosphate salt in chloroform is shown.

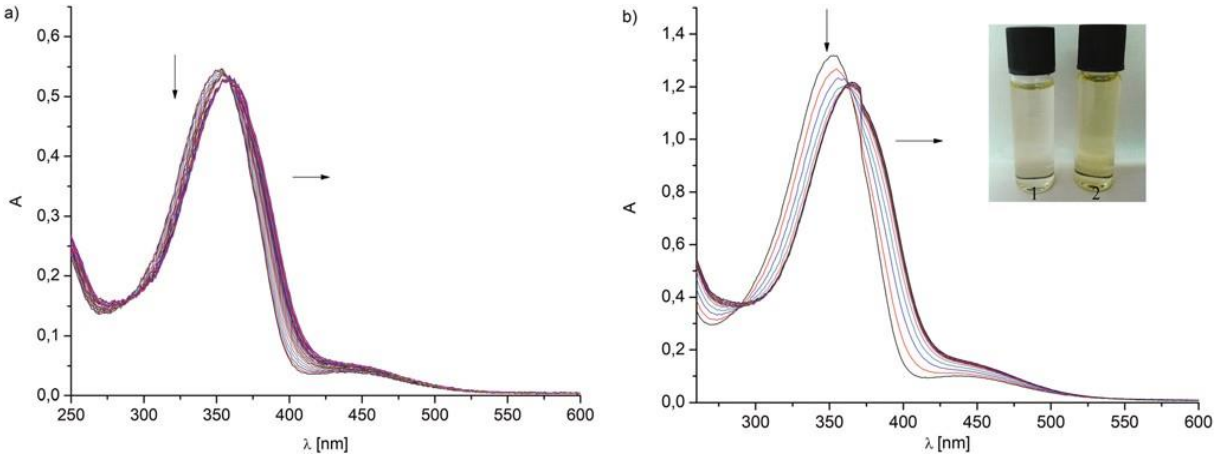


**Fig. 3** Changes in the UV-Vis spectra upon titration of the ligand (a) **3** ($c_3$ = 1.49 × $10^{-5}$ M, 0 ≤ R ≤ 37.78) and (b) **4** ($c_4$ = 1.37 × $10^{-5}$ M, 0 ≤ R ≤ 10.75) with tetra-*n*-butylammonium dihydrogen phosphate in chloroform; R: salt/ligand molar ratio; photo: 1 – ligand **4** in chloroform, and 2 – ligand **4** with an equimolar amount of dihydrogen phosphate salt in chloroform.

According to molar ratio plots (Fig. ESI2†) it can be concluded that for both ligands **3** and **4** equilibrium is reached at an equimolar ratio of ligand to salt. This suggests 1 : 1 complex type formation under these measurement conditions. On the basis of titration data, the values of the stability constants for ligands **3** and **4** were evaluated using OPIUM software

and compared (Fig. 4). In general, tripodal amide **4** forms more stable complexes with anions than dipodal derivative **3**, with the highest value for fluorides and chlorides. However, the effect of the tripodal platform is the most significant in the case of acetates, where the difference in the stability constant values (Δlog K) between complexes of **3** and **4** is 1.26. The values of the stability constants determined for complexes of amide **3** or **4** with halide ions decrease with an increase in ion size. Among all the tested anions, ligand **3** shows the highest affinity to spherical fluoride anions and tetrahedral, hydrophilic dihydrogen phosphate ions. The stronger affinity of amide **4**, than dipodal ligand **3**, to anions may be explained in two ways. The presence of the third amide arm in compound **4**, due to its –M and –I effects on the central benzene ring, causes a change in the electron density distribution, which increases the partial positive charge on the carbon atom between the two amide arms in the para position in relation to the third arm and decreases the electron density on the nitrogen atom making the neighboring amide hydrogen more acidic. This effect facilitates interactions with negatively charged species. Moreover, tripodal amide **4**, as it can be seen in models of 3 and 4 in Fig. 5, is preorganized for ion binding, forming a pseudo-cavity between the two amide arms (marked with a red circle). All amide residues in ligands **3** and **4** remain in the coplanar position with the central benzene ring. If the anion is complexed by two amide moieties in an appropriate conformation, statistically for tripodal compound **4** there is a higher probability of such interaction. In conclusion, stronger binding of anions by tripodal amide **4** can be explained by the additive and cooperative action of multiple factors, being a result of the electronic effect of the third amide residue (–M and –I), the probable conformation of the amide and statistical factors.

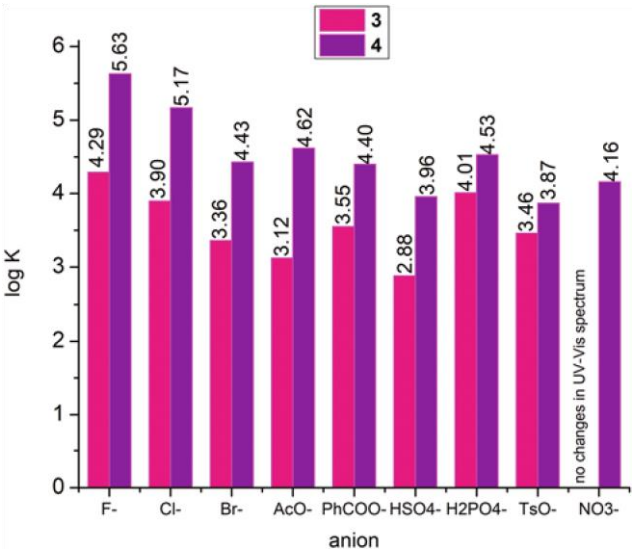


**Fig. 4** Comparison of the stability constant values log K of complexes (1 : 1) determined for ligands **3** and **4** with anions (as TBA salts) in chloroform.

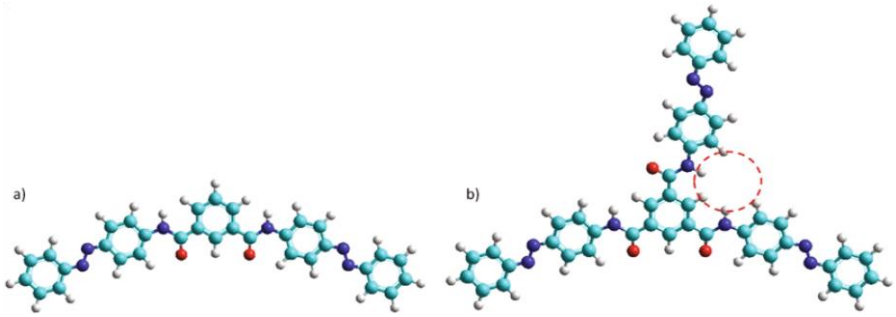


**Fig. 5** A comparison of molecular models of (a) dipodal amide **3** and (b) tripodal amide **4** by using the MM: UFF method. Red circle: proposed binding site.

As amide **4** interacts with the tested anions stronger than dipodal ligand **3**, other experiments were carried out for the derivative of trimesic acid **4**. The process of molecular recognition was investigated using $^{1}$H NMR spectroscopy on the example of interactions between amide **4** and tetra-*n*-butylammonium benzoate in chloroform-*d* (Fig. 6).

In the spectra below, it can be seen that the presence of a benzoate ion causes a significant shift and broadening of the signal assigned to the protons of the amide groups towards higher ppm values (Δδ = +1.65 ppm). This can indicate the formation of hydrogen bonds between the NH– groups of the ligand and anion. Signals of protons from the benzene platform marked as A are also shifted to higher ppm values (Δδ = +0.21 ppm), which may suggest the influence of potentially forming hydrogen bonds

on these protons. In the **4**-PhCOO⁻ complex spectrum, aromatic proton signals marked as B and C are also shifted (Δδ: +0.14 and +0.13 ppm respectively).

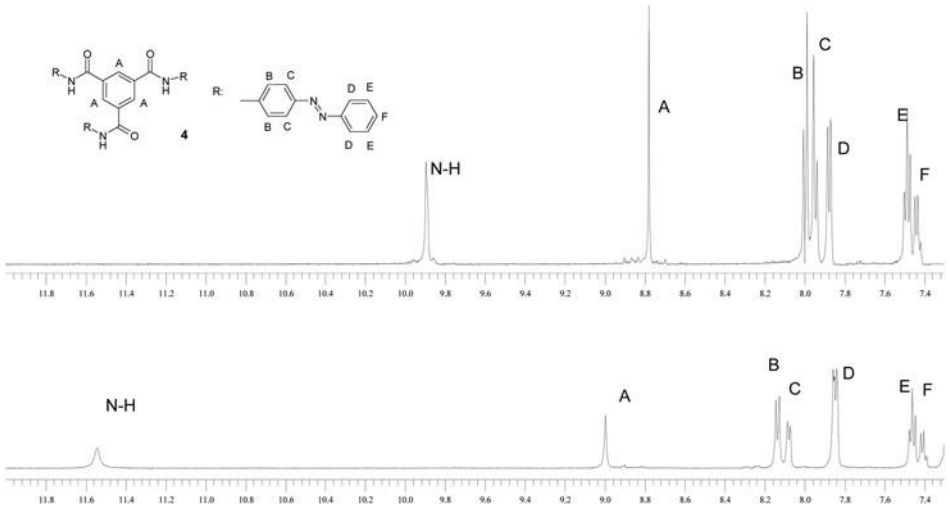


**Fig. 6** A comparison of the partial $^{1}$H NMR spectra of free ligand **4** (top) and its complex (1 : 1) with tetra-*n*-butylammonium benzoate (bottom) in chloroform-*d*.

Additional information regarding the nature of the tripodal ligand **4**-PhCOO⁻ interactions was acquired by FTIR spectroscopy (Fig. 7). The most significant spectral changes are observed in the region of the amide bands. The amide I band (*ν*C=O) in the complex is shifted towards higher frequencies (+12 cm$^{-1}$) in relation to the "free" ligand. The amide II band, resulting mostly from δN–H bending and *ν*C–N stretching vibrations, is shifted from 1530 cm$^{-1}$ in the free ligand to 1537 cm$^{-1}$. These changes suggest hydrogen bond formation between the amide N–H protons and the anion. The band of the (*ν*C=C) aromatic ring vibration (at ~1600 cm$^{-1}$) is not changed due to the ligand–ion interactions, which may indicate that the changes observed in the $^{1}$H NMR spectra are a consequence of hydrogen bond occurrence.

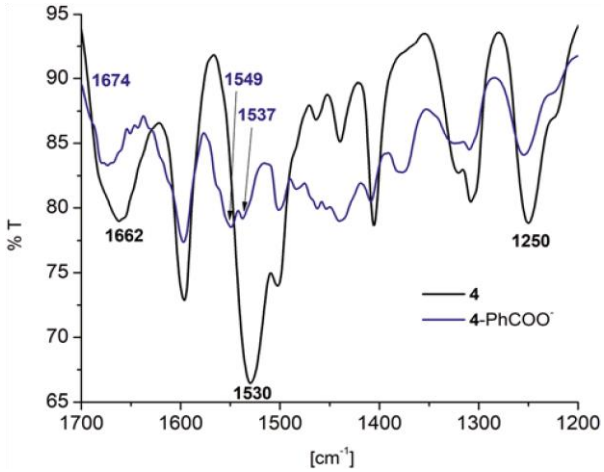


**Fig. 7** A comparison of the partial (1700-1200 $cm^{-1}$) FTIR spectra (KBr pellet) of **4** and its complex with tetra-*n*-butylammonium benzoate (1 : 1).

$^1$H NMR spectra of the amide **4** solution were also registered in the presence of tetra-*n*-butylammonium fluoride and nitrate in chloroform-*d* (Fig. ESI3†). Similar to the case of benzoate ions, the presence of fluoride or nitrate anions causes a shift of the amide proton signals to higher ppm values, which indicates the formation of hydrogen bonds between ligand **4** and the tested anions (Table 1). Taking into account the chemical shift values of these signals, it can be concluded that amide **4** forms stronger hydrogen bonds with fluoride ions than with nitrate, which is in accordance with the stability constant values determined from spectrophotometric titrations (log K: $F^- > PhCOO^- > NO_3^-$). In the **4**-$F^-$ spectrum (Fig. ESI3†), two broadened signals of NH protons are observed, whereas in the spectrum of the free ligand, these protons occur as one singlet. This may indicate the different involvement of the NH group in the guest coordination or slow proton exchange under the measurement conditions. Signals of protons from the benzene platform (labeled as A analogously to Fig. 6) seen in the spectrum of the "free" ligand solution as one singlet, in the **4**-$F^-$ spectrum, similarly to the NH proton signals, are observed as two separated singlets shifted towards higher ppm values in comparison to the free ligand spectrum.

**Table 1** The position of the signals of selected protons in the $^1$H NMR spectrum of the free amide **4** and its complexes with tetra-*n*-butylammonium fluoride and nitrate in chloroform-*d* (values in ppm; symbols as in Fig. 6: A – protons of the aromatic ring derived from carboxylic acid; B and C – protons of the aromatic ring between the amide and azo groups; * signals cannot be clearly assigned)

| | NH ($\Delta\delta$) | A | B | C |
|---|---|---|---|---|
| **4** | 9.90 | 8.78 | 8.00 | 7.95 |
| **4**-$NO_3^-$ | 10.24 (+0.34) | 8.57 | * | * |
| **4**-$F^-$ | 11.21; 10.51 (+1.31); (+0.61) | 9.27; 8.37 | 8.35 | 8.21 |

Analysis of the FTIR spectra provides additional information regarding the binding of fluoride ions by ligand **4**. In the **4**-$F^-$ spectrum, the amide I band is in the form of two slightly separated bands. In the free ligand spectrum, one band exists in the range of ($\nu$C=O) vibration (Fig. ESI4a†). The amide II band in the complex spectrum is shifted to higher wavenumber values ($\Delta\nu$ = 10 $cm^{-1}$), which suggests the formation of hydrogen bonds between the ligand and fluoride anion. Similar character of the changes in the spectrum of **4**-$NO_3^-$ is observed (Fig. ESI4b†). Both the amide I and II bands are shifted to higher wavenumber values in comparison to the free amide spectrum ($\Delta\nu$: 14 and 5 $cm^{-1}$, respectively).

The presence of electroactive azo groups in the structures of amides **1–4** makes them potential materials for electrochemical sensors. In order to test the electrochemical response towards anions, cyclic voltammetry was performed for the most interesting tripodal ligand **4**. The cyclic voltammetric curve registered for the ligand **4** solution in acetonitrile indicates the presence of well seen oxidation peak at −0.39 V and a reduction peak at −0.60 V. Changes in the formal potential of the ligand **4** solution in the presence of anions of different sizes and shapes (as TBA salts) are listed in Table 2.

**Table 2** Formal potential values of free ligand **4** solution ($c_4$ = 2.48 × $10^{-4}$ M) and ligand **4** in the presence of a 100-fold molar excess of TBA compounds in acetonitrile ($\Delta E^O = E^O_{complex} - E^O_{freeligand}$ mV *vs.* Ag/AgCl, KCl: c = 0.1 M)

| | **4** | $F^-$ | $Cl^-$ | $Br^-$ | $PhCOO^-$ | $H_2PO_4^-$ | $OH^-$ | $NO_3^-$ | $HSO_4^-$ |
|---|---|---|---|---|---|---|---|---|---|
| $E^O$ ($\Delta E^O$) [mV *vs.* Ag/AgCl] | -495 | -426 (69) | -484 (11) | -496 (1) | -519 (-24) | -539 (-44) | -506 (-11) | -465 (30) | -443 (52) |

Anion complexation by receptors with electroactive moieties is mostly connected with a shift of the cyclic voltammetry curve to lower potential values.[20] This effect in the voltammogram of amide **4** solution is observed in the presence of tetra-*n*-butylammonium hydroxide, benzoate, and dihydrogen phosphate. The values of cathodic shift decrease in the order of ΔE°: $H_2PO_4^-$ > $PhCOO^-$ > $OH^-$, which is in agreement with the increase in the anion basicity. Different character of changes are observed in the presence of halides, nitrates, and hydrogen sulfates. In these cases, the cyclic voltammetry curves of the ligand solution are shifted to higher potential values. Among the tested halide ions, the largest anodic shift is caused by the smallest fluoride anions. The ΔE° values decrease with an increase in the halide ionic radius, which correlates with the stability constant values obtained from spectrophotometric titrations, despite the significant difference in the properties of the solvents applied in both experiments. As an example, a comparison of the voltammograms registered for the free amide **4** and **4** in the presence of dihydrogen phosphate ions is shown in Fig. 8.

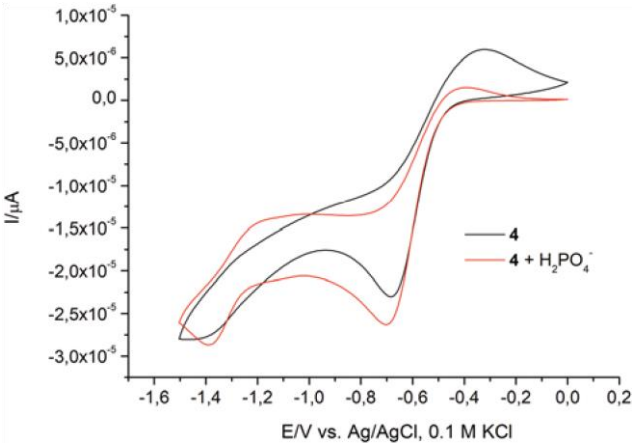


**Fig. 8.** A comparison of the cyclic voltammetry curves of the free ligand **4** solution ($c_4$ = 2.48 × $10^{-4}$ M) and ligand **4** in the presence of a 100-fold molar excess of tetra-*n*-butylammonium dihydrogen phosphate in acetonitrile (electrolyte: 0.1 M tetra-*n*-butylammonium perchlorate).

Azo compounds may exist in the form of two isomers: *E* (*trans*) and *Z* (*cis*). The photoisomerization process was studied for the most promising compound, **4**, dissolved in chloroform. In the UV-Vis spectra (Fig. 9a) showing *E* to *Z* isomerization induced by UV irradiation, two isosbestic points are observed, which may indicate that only one process takes place: *trans* to *cis* isomerization. After sample irradiation (at intervals of 30 seconds) hypsochromic shift of the π → π* band and hyperchromic shift

of the *n* → π* band are observed, until the photostationary state is reached. Using a graphical method (drawing the relationship of ln $c_4$ vs. time), it was determined that UV induced isomerization is a first-order reaction (Fig. ESI5†). The reverse process – *Z* to *E* isomerization – was carried out in the dark at 50 °C (Fig. 9b). In the UV-Vis spectrum of the solution of the *Z* isomer, batho- and hyperchromic shift of the π → π* band and hypochromic shift of the n →π* band are observed. After 80 minutes of heating the solution in the dark, the *E* isomer dominates in solution. According to the graph (Fig. ESI6†), the thermal back reaction is a first order process with a half-life time of 24 minutes. The process of *Z* ⇄ *E* isomerization of **4** was also studied in DMSO.[21]

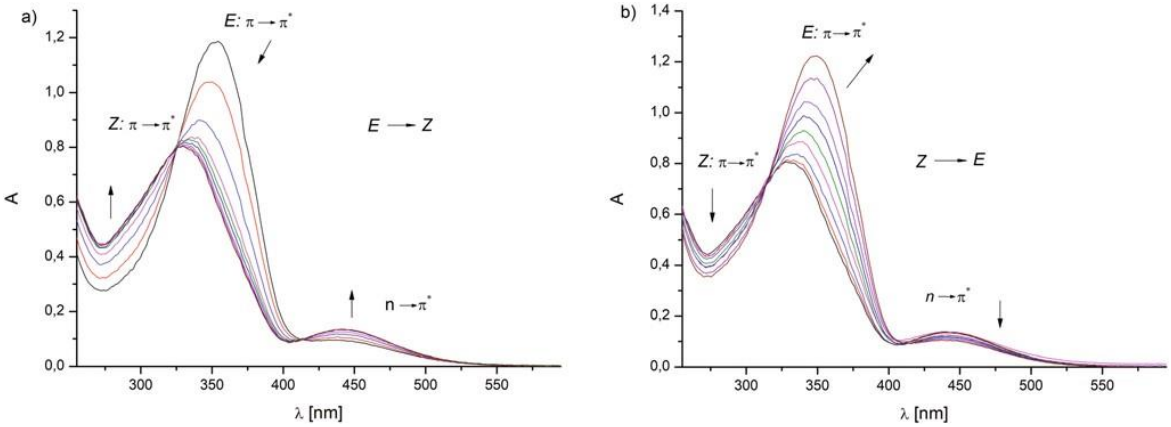


**Fig. 9** Changes in the UV-Vis spectra of a ligand **4** solution ($c_4$ = 2.01 × $10^{-5}$ M) in chloroform during (a) irradiation with a UVA lamp ($\lambda_{max}$ = 365 nm) and (b) heating at 50 °C in the dark. Arrows indicate the direction of spectral changes.

As ligand **4** in its E form interacts with anions, the affinity of the *Z* isomer to anions was also checked (Table 3). Addition of anionic species to a *Z*-**4** solution accelerates the rate of *Z* to *E* thermal isomerization. This effect seems to be dependent on the type of added TBA salt and can be rationalized by the strength of ligand **4**–anion interactions determined for its *trans* form (Fig. 4). The fluorides most strongly bound by E-**4** cause the largest bathochromic shift of the *Z* π → π* band and have the highest impact on the acceleration of the thermal back reaction among all the tested anions. A shown in Table 3, the time required for the formation of the *E* isomer is 10-fold shorter in the presence of fluoride ions than in the absence of anionic species. This can be explained by the fact that interaction with anions increases the electron density on the $-\overline{N}=\overline{N}-$ moiety of the receptor, and as a consequence increases the repulsion

between the lone pairs of the azo group. This leads to a decrease in the thermal isomerization barrier and shortening of the thermal back reaction time. Similar observations were described for urea derivatives bearing azo groups, for which *cis* to *trans* isomerization could be accelerated by the addition of particular anions.[22] On the other hand, Shinkai et al.[23] showed that the presence of certain cations suppresses the thermal isomerization of crown ethers bearing azo units.

**Table 3** Spectral and kinetic data of *Z* → *E* thermal isomerization of the *Z*-**4** complex with 100 eq. of selected tetra-*n*-butylammonium salts in chloroform; $\Delta^{\lambda}_{\pi} \rightarrow \pi^*$ – shift of the maximum absorption of free *Z*-**4** and its complexes with anions

| | $F^-$ | $AcO^-$ | $PhCOO^-$ |
|---|---|---|---|
| *t* [min] | 8 | 10 | 15 |
| $\Delta\lambda_{\pi\rightarrow\pi^*}$ [nm] | 12 | 10 | 8 |

## Conclusions

We described a facile synthesis of *p*-aminoazobenzene-derived acyclic compounds bearing one, two or three amide moieties. Among the obtained amides, one compound – ligand **2** – which is a derivative of pyridine-2,6-dicarboxylic acid has not been described in the literature before. Di- and tripodal receptors **3** and **4** derived from isophthalic and trimesic acids show affinity to several anions forming 1 : 1 type complexes in chloroform. Tripodal ligand **4** interacts with anions stronger than its dipodal analogue **3**. Incorporation of azo groups into the ligand structures enables optical and electrochemical anion recognition. Thermal *Z* to *E* isomerization of amide **4** is accelerated in the presence of anionic species. The effect of acceleration is connected with anion complementarity to the host molecule.

## Conflicts of interest

There are no conflicts to declare.

## Acknowledgements

The authors kindly acknowledge support from sources for science GUT Grants No. 031841 and 032406. The authors also thank Prof. Elżbieta Luboch and Prof. Jan F. Biernat

for fruitful discussion, student Marta Hewelt for her experimental contribution and Koleta Majewska, MSc for technical support in the manuscript preparation. The authors thank the anonymous reviewers for their careful review, which helped to improve the quality of the above manuscript.

## References

1. (a) P. A. Gale, E. N. W. Howe and X. Wu, Anion receptor chemistry, Chemistry, 2016, 1, 351–422; (b) S. K. Sahho, G.-D. Kim and H.-J. Choi, Optical sensing of anions using $C_{3v}$-symmetric tripodal receptors, J. Photochem. Photobiol., C, 2016, 27, 30–53.
2. (a) A. M. Wilson, P. J. Bailey, P. A. Tasker, J. R. Turkington, R. A. Grant and J. B. Love, Solvent Extraction: the coordination chemistry behind extractive metallurgy, Chem. Soc. Rev., 2014, 43, 123–134; (b) R. Alberto, G. Bergamaschi, H. Braband, T. Vox and V. Amendola, $^{99}TcO_4^-$: Selective recognition and trapping in aqueous solutions, Angew. Chem., Int. Ed., 2012, 51, 9772–9776.
3. (a) N. Busschaert, C. Caltagirone, W. Van Rossom and P. A. Gale, Applications of supramolecular anion recognition, Chem. Rev., 2015, 115, 8038–8155; (b) D. Yuan, H. C. Anthis, M. G. Afshar, N. Pankratova, M. Cuartero, G. A. Crespo and E. Bakker, All-solid-state potentiometric sensors with a multiwalled carbon nanotube inner transducing layer for anion detection in environmental samples, Anal. Chem., 2015, 87, 8640–8645.
4. (a) I. T. Raheem, P. S. Thiara, E. A. Peterson and E. N. Jacobsen, Enantioselective Pictet-Spengler-type cyclizations of hydroxylactams: H-bond donor catalysis of anion binding, J. Am. Chem. Soc., 2007, 129, 13404–13405; (b) G. Bergonzini, C. S. Schindler, C.-J. Wallentin, E. N. Jacobsen and C. R. J. Stephenson, Chemical science photoredox activation and anion binding catalysis in the dual catalytic enantioselective synthesis of β-aminoesters, Chem. Sci., 2014, 5, 112–116.
5. (a) H. Miyaji and J. L. Sessler, Off-the-shelf colorimetric anion sensors, Angew. Chem., Int. Ed., 2001, 40, 154–157; (b) P. A. Gale and C. Caltagirone, Anion sensing by small molecules and molecular ensembles, Chem. Soc. Rev., 2015, 44, 4212–4227.
6. (a) E. Merino, Synthesis of azobenzenes: the coloured pieces of molecular materials, Chem. Soc. Rev., 2011, 40, 3835–3853; (b) E. Léonard, F. Mangin, C. Villette, M. Billamboz and C. Len, Azobenzenes and catalysis, Catal. Sci. Technol., 2016, 6, 379–398;

(c) F. Hamon, F. DjedainiPilard, F. Barbot and C. Len, Azobenzenes – synthesis and carbohydrate applications, Tetrahedron, 2009, 65, 10105– 10123.

7. (a) C. García-Iriepa, M. Marazzi, L. M. Frutos and D. Sampedro, E/Z Photochemical switches: syntheses, properties and applications, RSC Adv., 2013, 3, 6241–6266; (b) R. Ahmed, A. Priimagi, C. F. J. Faul and I. Manners, Redox-active, organometallic surface-relief gratings from azobenzene-containing polyferrocenylsilane block copolymers, Adv. Mater., 2012, 24, 926–931; (c) A. A. Beharry, O. Sadovski and G. A. Woolley, Azobenzene photoswitching without ultraviolet light, J. Am. Chem. Soc., 2011, 133, 19684–19687; (d) M. Dong, A. Babalhavaeji, S. Samanta, A. A. Beharry and G. A. Woolley, Red-shifting azobenzene photoswitches for in vivo use, Acc. Chem. Res., 2015, 48, 2662–2670; (e) R. Reuter and H. A. Wegner, Oligoazobenzenophanes - synthesis, photochemistry and properties, Chem. Commun., 2011, 47, 12267–12276; (f) I. Zawisza, R. Bilewicz, E. Luboch and J. F. Biernat, Complexation of metal ions by azocrown ethers in Langmuir-Blodgett monolayers, J. Chem. Soc., Dalton Trans., 2000, 4, 499–503.
8. (a) E. Luboch, R. Bilewicz, M. Kowalczyk, E. WagnerWysiecka and J. F. Biernat, Azo Macrocyclic Compounds, in Advances in Supramolecular Chemistry, ed. G. W. Gokel, Cerberus Press, Inc., South Miami, 2003, vol. 9, pp. 73–163; (b) Z. Li, J. Liang, W. Xue, G. Liu, S. H. Liu and J. Yin, Switchable azo-macrocycles: from molecules to functionalization, Supramol. Chem., 2014, 26, 54–65; (c) E. Luboch, J. F. Biernat, E. Muszalska and R. Bilewicz, 13-Membered crown ethers with azo or azoxy unit in the macrocyclesynthesis, membrane electrodes, voltammetry and Langmuir monolayers, Supramol. Chem., 1995, 5, 201–210; (d) E. Luboch, J. F. Biernat, Y. A. Simonov and A. A. Dvorkin, Synthesis and electrode properties of 16-membered azo- and azoxycrown ethers. Structure of tribenzo-16-azocrown-6, Tetrahedron, 1998, 54, 4977–4990; (e) E. Luboch, E. Wagner-Wysiecka and J. F. Biernat, Chromogenic azocrown ethers with peripheral alkyl, alkoxy, hydroxy or dimethylamino group, J. Supramol. Chem., 2002, 2, 279–291; (f) E. Luboch, E. WagnerWysiecka, Z. Poleska-Muchlado and V. C. Kravtsov, Synthesis and properties of azobenzocrown ethers with π-electron donor, or π-electron donor and π-electron acceptor group(s) on benzene ring(s), Tetrahedron, 2005, 61, 10738–10747; (g) E. Luboch, E. Wagner-Wysiecka and T. Rzymowski, 4-Hexylresorcinol-derived hydroxyazobenzocrown ethers as chromoionophores, Tetrahedron, 2009, 65,

10671–10678; (h) E. Wagner-Wysiecka, T. Rzymowski, M. Szarmach, M. S. Fonari and E. Luboch, Functionalized azobenzocrown ethers as sensor materials -the synthesis and ion binding properties, Sens. Actuators., B, 2013, 177, 913–923; (i) M. Szarmach, E. Wagner-Wysiecka and E. Luboch, Rearrangement of azoxybenzocrowns into chromophoric hydroxyazobenzocrowns and the use of hydroxyazobenzocrowns for the synthesis of ionophoric biscrown compounds, Tetrahedron, 2013, 69, 10893–10905; (j) E. Luboch, M. Szarmach, M. Jeszke and N. Łukasik, New bis(azobenzocrown)s with dodecylmethylmalonyl linkers as ionophores for sodium selective potentiometric sensors, J. Inclusion Phenom. Macrocyclic Chem., 2016, 86, 323–335; (k) E. Wagner-Wysiecka, M. Szarmach, J. Chojnacki, N. Łukasik and E. Luboch, Cation sensing by diphenylazobenzocrowns, J. Photochem. Photobiol., A, 2017, 333, 220–232.

9. M. Banghart, K. Borges, E. Isacoff, D. Trauner and R. H. Kramer, Light-activated ion channels for remote control of neuronal firing, Nat. Neurosci., 2004, 7, 1381– 1386.
10. W. C. Lin, C. M. Davenport, A. Mourot, D. Vytla, C. M. Smith, K. A. Medeiros, J. J. Chambers and R. H. Kramer, Engineering a light-regulated GABA(A) receptor for optical control of neural inhibition, ACS Chem. Biol., 2014, 9, 1414–1419.
11. M. Ali, M. W. Forbes and G. A. Woolley, Optimizing the photocontrol of bZIP coiled coils with azobenzene crosslinkers: role of the crosslinking site, ChemBioChem, 2015, 16, 1757–1763.
12. (a) J. García-Amorós and D. Velasco, Recent advances towards azobenzene-based light-driven real-time information-transmitting materials, Beilstein J. Org. Chem., 2012, 8, 1003–1017; (b) T. Avellini, H. Li, A. Coskun, G. Barin, A. Trabolsi, A. N. Basuray, S. K. Dey, A. Credi, S. Silvi, J. F. Stoddart and M. Venturi, Photoinduced memory effect in a redox controllable bistable mechanical molecular switch, Angew. Chem., Int. Ed., 2012, 51, 1611– 1615; (c) E. Merino and M. Ribagorda, Control over molecular motion using the cis-trans photoisomerization of the azo group, Beilstein J. Org. Chem., 2012, 8, 1071–1090; (d) H. M. D. Bandara and S. C. Burdette, Photoisomerization in different classes of azobenzene, Chem. Soc. Rev., 2012, 41, 1809–1825.
13. (a) E. Wagner-Wysiecka and N. Łukasik, Anion recognition by N,N'-diarylalkanediamides, Tetrahedron Lett., 2012, 53, 6029–6034; (b) E. Wagner-Wysiecka and J. Chojnacki, Chromogenic amides of pyridine-2,6-dicarboxylic acid as anion receptors, Supramol. Chem., 2012, 24, 684–695; (c) N. Łukasik, E. Wagner-Wysiecka, V.

Hubscher-Bruder, S. Michel, M. Bocheńska and B. Kamińska, Naphthyl- vs. anthrylpyridine-2,6-dicarboxamides in cation binding studies. Synthesis and spectroscopic properties, Supramol. Chem., 2016, 28, 673–685.

14. Y. Li, Y. Wang and J. Wang, Microwave-assisted synthesis of amides from various amines and benzoyl chloride under solvent-free conditions: a rapid and efficient method for selective protection of diverse amines, Russ. J. Org. Chem., 2008, 44, 358–361.
15. L. M. Goldenberg, L. Kulikovsky, O. Kulikovska, J. Tomczyk and J. Stumpe, Thin layers of low molecular azobenzene materials with effective light-induced mass transport, Langmuir, 2010, 26, 2214–2217.
16. M. Kyvala and I. Lukeš, program package "OPIUM" available (free of charge) at http://www.natur.cuni.cz/~kyvala/ opium.html.
17. M. Thompson, program package "ArusLab" available (free of charge) at http://www.arguslab.com/arguslab.com/ ArgusLab.html.
18. K. Iwato, Composition for forming low-dielectric-constant film, insulating film, and electronic device, US 2008/ 0161532Al, 2008.
19. S. Lee, S. Oh, J. Lee, Y. Malpani, Y.-S. Jung, B. Kang, J. Y. Lee, K. Ozasa, T. Isoshima, S. Y. Lee, M. Hara, D. Hashizume and J.-M. Kim, Stimulus-responsive azobenzene supramolecules: fibres, gels, and hollow spheres, Langmuir, 2013, 29, 5869–5877.
20. (a) P. D. Beer, P. A. Gale and G. Z. Chen, Mechanisms of electrochemical recognition of cations, anions and neutral guest species by redox-active receptor molecules, Coord. Chem. Rev., 1999, 185–186, 3–36; (b) K. Kaur, S. K. Mittal, S. K. Ashok Kumar, A. Kumar and S. Kumar, Viologen substituted anthrone derivatives for selective detection of cyanide ions using voltammetry, Anal. Methods, 2013, 5, 5565–5571.
21. J. Kind, L. Kaltschnee, M. Layendecker and C. M. Thiele, Distinction of trans-cis, photoisomers with comparable optical properties in multiple-state photochromic systems – examining a molecule with three azobenzenes via in situ irradiation NMR spectroscopy, Chem. Commun., 2016, 52, 12506–12509.
22. K. Dąbrowa, P. Niedbała and J. Jurczak, Anion-tunable control of thermal Z→E isomerization in basic azobenzene receptors, Chem. Commun., 2014, 50, 15748–15751.
23. S. Shinkai, T. Nakaji, T. Ogawa, K. Shigematsu and O. Manabe, Photoresponsive crown ethers. 2. Photocontrol of ion extraction and ion-transport by a bis(crown ether) with a butterfly-like motion, J. Am. Chem. Soc., 1981, 103, 111–115.